Texture Feature Coding Method for Classification of Liver Sonography

Ming-Huwi Horng[1] , Yung-Nien Sun[1] and Xi-Zhang Lin[2]
[1]Institute of Information Engineering,[2]Department of Internal Medicine, National Cheng Kung University, Tainan, Taiwan, R.O.C.

Abstract Liver sonography is a widely used noninvasive diagnostic tool. Analyzing histology changes in sonograms provides a means of diagnosing and monitoring chronic liver diseases. Nonetheless, conventional ultrasonography is still qualitative. To improve reliability of liver diagnosis, quantitative image analysis is highly desirable for the assessment of various liver states. In this paper, a novel approach, called Texture Feature Coding Method (TFCM) is presented for texture classification of liver sonography, more specifically, classification of normal liver, hepatitis and cirrhosis. TFCM is a texture analysis technique based on gray-level gradient variations in a 3x3 texture unit. It transforms an image into a texture feature image in which each pixel is represented by a texture feature number (*TFN*) coded by TFCM. The obtained texture feature numbers are then used to generate a *TFN* histogram and a *TFN* co-occurrence matrix which will produce texture feature descriptors. By coupling with a supervised maximum likelihood (ML) classifier, these descriptors form a classification system to discriminate the three above-mentioned liver classes. The TFCM-supervised ML system is trained by 30 liver samples proven by biopsy and tested on a set of 90 samples. The results show that the designed *TFN*-supervised ML system performs better than do existing techniques, and the correct classification rate can reach as high as 83.3%.

1. Introduction

In chronic liver diseases the severity of infected patients may range from healthy carrier to cirrhosis. In the past literature, several characteristics have been used to evaluate diffuse parenchyma liver diseases in past literature [2-4]. These include changes in echotexture, echogenicity, liver surface, inferior edge, diameter of hepatic duct and cystic vein. Of particular interest are the changes of echotexture. But the quality of the ultrasonic liver images is very poor since some images properties, such as edgeness, coarseness, etc., are severely affected by various noises. According to clinical experts, the liver histological changes from normal to cirrhosis can be described by the gray-level gradient variation of the echotexture in ultrasonic liver images. Thus, if we can establish correlation between gray-level gradient variations in echotexture and liver histology, using this information will be of great advantage for liver sonography analysis because it not only can assist physicians in diagnosis of liver diseases, but also provides assessment of progressive development of liver diseases.

Over the past several years a number of approaches have been proposed in natural texture classification. Among them are the gray-level co-occurrence matrix [1], statistical feature matrix [5] and texture spectrum [6] which are the most interesting texture analysis techniques that can be applied to liver images. However, these approaches do not produce satisfactory results. To improve their performance,

a novel approach to texture analysis for liver sonography, called **T**exture **F**eature **C**oding **M**ethod (TFCM) is presented in this paper, particularly, for classification of three liver states, normal liver, hepatitis, cirrhosis. TFCM is a coding scheme which transforms an image into a texture feature image in which each pixel is encoded by TFCM into a texture feature number (*TFN*) which represents a certain type of local texture. In order to discriminate subtle details of a texture, the ideas of gray-level histogram and co-occurrence matrix are introduced into TFCM, called a texture feature number histogram and a texture feature number co-occurrence matrix respectively from which a set of texture feature number (*TFN*) descriptors are generated for texture classification. Finally, these *TFN* descriptors are coupled with a supervised maximum likelihood (ML) classifier to form a TFCM system consisting of *TFN* descriptors and a supervised ML classifier for liver sonography. The results show that the system outperforms existing methods and the correct classification rate can reach as high as 83.3%.

V_2	V_3	V_4
V_1	V_0	V_5
V_8	V_7	V_6

Figure1. Texture unit of texture spectrum

2	1	2
1	X	1
2	1	2

Figure 2. Texture unit of TFCM

2. Texture Feature Coding Method

In this section, we propose a novel approach to generating texture feature numbers, called **T**exture **F**eature **C**oding **M**ethod (TFCM). The design rationale of this method is based on gray-level gradient variations of a 3×3 texture unit.

2.1 Texture Feature Number Generation

2.1.1 Texture Unit

TFCM is a coding scheme which transforms an original image into a texture feature image whose pixels are represented by texture feature numbers coded by TFCM. The texture feature number of each pixel **X** is generated on the basis of gray-level changes of its 8 surrounding pixels, called a texture unit, a term was in He and Wang's work [6] described in Figure 1. Unlike He and Wang's texture spectrum, we consider the connectivity of a texture unit.

2.1.2. First-order and Second-order Connectivity of A Texture Unit

The 8 neighboring pixels in Figure 2 constitute the 8-connectivity of the texture unit which can be divided into the first-order 4-connectivity pixels and second-order 4-connectivity pixels. The four pixels labelled by **1** satisfy the first-order 4-connectivity of the texture unit because they are immediately adjacent to the pixel **X**. They will be denoted by first-order connectivity pixels. The other four pixels labelled by **2** satisfy the second-order 4-connectivity of the texture unit which

are diagonally adjacent to **X** and will be denoted by second-order connectivity pixels. In general, first-order connectivity pixels have higher correlation with pixel **X** than do second-order connectivity pixels.

2.1.3 Scan Lines of First-order and Second-order

In order to code pixel **X** in Figure 2, TFCM produces a pair of integers (α,β) where α and β represent gray-level gradient variations of three successive first-order connectivity and second-order connectivity pixels respectively. As shown in Figure 3, two scan lines along 0^o-180^o and 90^o-270^o directions produce two sets of three successive first-order connectivity pixels with pixel **X** in the middle which are horizontal line and vertical line denoted by "+". Similarly, two scan lines along diagonal direction 45^o-225^o and asymmetric diagonal direction 135^o-315^o denoted by "×" also produce two sets of three successive second-order connectivity pixels as shown in Figure 4. The α and β will be used to indicate types of the gray-level gradient variations between pixels (*a* and *b*) and (*b* and *c*) described below in equation (1) or Figure 5.

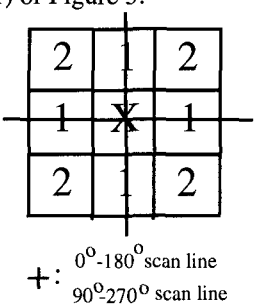

Figure 3. First-order 4-connectivity

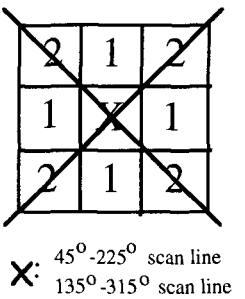

Figure 4. Second-order 4-connectivity

In other words, each pixel in an original image will be coded by a pair of (α, β) based on types of gray-level gradient variations using the first-order connectivity and second-order connectivity pixels of its texture unit.

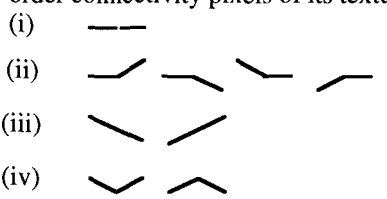

Figure 5. Types of gray-level graphical structure gradient variation

2.1.4 Types of Gray-Level Gradient Variation of a Texture Unit

Suppose that (G_a,G_b,G_c) corresponds the gray levels of three pixels (a,b,c) respectively. The two successive gray-level changes between two pairs (G_a,G_b) and (G_b,G_c) form four different types of variations. Let Δ be a tolerance of variation. Type (i) describes the case that the gray levels of *a*, *b* and *c* are very close within the tolerance Δ. Type (ii) is the case that one pair of gray levels are very close within

Δ, but the other pair is not and its gray-level gradient variation exceeds Δ. Type (iii) is the case that the gray levels of a,b,c are continuously decreasing or increasing with gray-level differences larger than Δ. Type (iv) is the most drastic case that either the gray-level variation is first decreasing, then increasing or first increasing, then decreasing where all the increments and decrements in this type exceed Δ.

(i) *if* $(|G_a - G_b| \le \Delta) \cap (|G_b - G_c| \le \Delta)$

(ii) *if* $[(|G_a - G_b| \le \Delta) \cap (|G_b - G_c| \le \Delta)] \cup [(|G_a - G_b| \ge \Delta) \cap (|G_b - G_c| \le \Delta)]$

(iii) *if* $[(G_a - G_b > \Delta) \cap (G_b - G_c > \Delta)] \cup [(G_b - G_a > \Delta) \cap (G_c - G_b > \Delta)]$

(iv) *if* $[(G_a - G_b > \Delta) \cap (G_c - G_b > \Delta)] \cup [(G_b - G_a > \Delta) \cap (G_b - G_c > \Delta)]$ (1)

2.1.5 Types of Gray-Level Graphical Structure Gradient Variations

The four types of gray-level graphical structure gradient variations given by equation (1) can be graphed by the following gray-level graphical structure variations respectively.

Second-order 4-connectivity \ First-order 4-connectivity	(i)	(ii)	(iii)	(iv)
(i)	1	2	3	4
(ii)	2	5	6	7
(iii)	3	6	8	9
(iv)	4	7	9	10

Figure 6. Texture feature number generation table

According to the degree of gray-level graphical structure variation. The higher the order of graphical structure variation, the more the changes of gray-level are the larger the gray-level gradient variation.

Figure 6 is symmetric where the column represents the horizontal scan line 0^o-180^o for α and the diagonal line 45^o-225^o for β, and the row represents the vertical scan line 90^o-270^o for α and the asymmetric diagonal line 135^o-315^o for β. Finally, the texture feature number of each pixel is generated by taking the product of α and β. More precisely, let the gray level of the pixel with spatial location (x,y) be denoted by $G(x,y)$ and the corresponding texture feature number by $TFN(x,y)$. Then

$$TFN(x,y) = \alpha(x,y)\beta(x,y) \quad (2)$$

where $\alpha(x,y)$ and $\beta(x,y)$ are values obtained by Figure 6 for the pixel at spatial location (x,y). In order to find an optimal gray-level gradient variation tolerance Δ, we adopt the following *TFN* entropy definition as the criterion for optimality,

$$H_{TEN}(\Delta) = -\sum_{x}\sum_{y} p_{\Delta}(TFN(x,y)) \log p_{\Delta}(TFN(x,y)). \quad (3)$$

where (x,y) is taken over all pixels in the image. The optimal choice for Δ is obtained by finding the maximum entropy of equation (3). That is, let Δ^* be the optimal choice for Δ, then Δ^* satisfies

$$\Delta^* = \arg\{\max_{\Delta} H_{TEN}(\Delta)\}. \quad (4)$$

According to experiments, we have found that $\Delta^* = 3$ yielded the maximum entropy of equation (4).

2.2 Texture Feature Number Histogram

According to equation (4) $TFN(x,y)$ can take on 100 values ranging from 1 to 100. However, we can compress 100 values to 42 values by removing unused texture feature numbers, for instance, all prime numbers are removed since they cannot be decomposed into a product of two integers as shown in equation (2). By relabelling we can assume that these 42 values take on values from 0 to 41, i.e., $\{0,1,2,\ldots,41\}$. In this case, we can define a texture feature number histogram by

$$p_{\Delta}(n) = \frac{N_{\Delta}(n)}{N}, \quad n \in \{0,1,2,\ldots,41\} \quad (5)$$

where Δ is the gray-level gradient variation tolerance given in equation (1), $N_{\Delta}(n)$ is the frequency of occurrence of the texture feature number n and N is the total number of pixels in the feature image.

2.3 Texture Feature Number Co-occurrence Matrix

In the TFCM approach, we define a co-occurrence matrix on texture feature numbers of the feature image obtained by TFCM, called texture feature number co-occurrence matrix. In analogy with equation (1), a probability distribution of transitions between any pair of arbitrary two texture feature numbers can be defined similarly by

$$p_{\Delta}(i,j|d,\theta) = \frac{N_{\Delta d,\theta}(i,j)}{N_t}, \quad i,j \in \{0,1,2,\ldots,41\} \quad (6)$$

where Δ is the gray-level gradient variation tolerance given in equation (3), $N_{\Delta d,\theta}(i,j)$ is defined similarly as equation (1) with the gray-level gradient variation tolerance Δ, i and j are texture feature numbers rather than gray levels as defined in equation (1) and N_t is the normalization factor which is the total number of TFN transitions.

3. Texture Feature Descriptors

In what follows, we derive 8 texture feature descriptors based on definitions of equation (5) and equation (6). Of particular interest is the last descriptor which not only takes care of the joint occurrence of two TFNs, but also includes the pixel's

spatial location (x,y). Thus, we call it a second-order correlation descriptor because it accounts for *TFN*'s auto-correlation and *TFN*-spatial correlation.

1) Coarseness: $Coarse = \sum_{\Delta=0}^{R} p_{\Delta}(41)$ where R is a positive integer. A pixel corresponding to *TFN* 41 represents a drastic change in its 8-connectivity neighborhood. So, the total number of these *TFN*s also provides a good indication of coarseness.

2) Homogeneity: $Hom = \sum_{\Delta=0}^{R} p_{\Delta}(0)$. A pixel corresponding to *TFN* 0 represents no significant change in its 8-connectivity neighborhood. So, the total number of these *TFN*s provides a good indication of homogeneity.

3) Mean Convergence: $MC = \sum_{n=0}^{41} \frac{\left| n \cdot p_{\Delta}(n) - \mu_{\Delta} \right|}{\sigma_{\Delta}}$ This feature descriptor indicates how close the texture approximates the mean.

4) Variance: $Var = \sum_{n=0}^{41} (n-\mu_{\eta})^2 \cdot p_{\Delta}(n)$. The variance measures deviation of *TFN*s from the mean.

5) Entropy: $Entropy = -\sum_{i=0}^{41}\sum_{j=0}^{41} p_{\Delta}(i,j|d,\theta) \log p_{\Delta}(i,j|d,\theta)$ where $p_{\Delta}(i,j|d,\theta)$ is the (i,j)-th entry of the *TFN* co-occurrence matrix.

6) Run Length Density: $RLD = \sum_{i=1}^{41} p_{\Delta}^2(i,i|d,\theta)$ where $p_{\Delta}(i,j|d,\theta)$ is defined above with $i = j$. This feature descriptor is used to calculate the density of run length of *TFN*s in its 8-connectivity neighborhood.

7) Regularity: $Regularity = \sum_{i=0}^{41}\sum_{j=0}^{41} \frac{p_{\Delta}(i,j|d,\theta)}{1+(i-j)^2}$ This feature descriptor measures the regularity of *TFN*s. The higher the regularity number, the more close the *TFN*s in its 8-connectivity neighborhood.

8) Gray-Level Resolution Similarity: $GLRS = \sum_{i=0}^{41}\sum_{j=0}^{41} \frac{p(i,j|x,y)}{1+(i-j)^2}$. where $p(i,j|x,y)$ is defined as the joint probability of *TFN* i of the pixel (x,y) in the *TFN* co-occurrence matrix with $\Delta = 0$ and *TFN* j of the same pixel (x,y) in the *TFN* co-occurrence matrix with $\Delta^* = 3$. This feature descriptor provides information about the probability of a pixel at (x,y) whose *TFN* is i at $\Delta = 0$ and *TFN* j at $\Delta^* = 3$. The higher the *GLRS*, the less the change in *TFN*s of the same pixel, thus, the less change the gray levels in this neighborhood. Unlike feature descriptor (7), this feature descriptor includes the information of changes in gray levels from $\Delta = 0$ to $\Delta^* = 3$.

4. Supervised Maximum Likelihood Classification

In Section III, we introduced TFCM to generate a set of 8 texture feature descriptors which will be used for texture classification. The classification to be presented in this section is the well-known maximum likelihood classification. Suppose that K is the number classes of interest into which a set of samples will be classified. Let $p(x|\omega_i)$ be the conditional class probability distribution, viz., the probability of x given that x belongs to the class ω_i. A feature classifier is a decision function which assigns each feature to its associated class according to a certain criterion for optimality. A maximum likelihood (ML) feature classifier is a feature classifier designed based on the conditional class probability distribution $p(x|\omega_i)$ so that a feature x will be assigned to class ω_i if $p(x|\omega_i)$ yields largest probability among all K classes. More precisely,

$$x \in \omega_i \quad \text{if} \quad p(x|\omega_i) = \max_{j \in \{0,1,\ldots,K\}} p(x|\omega_j). \tag{7}$$

However, the ML classifier is *a priori* classification technique where the probability distribution $p(x|\omega_i)$ is assumed to be given. In many applications, $p(x|\omega_i)$ must be estimated by observations. As a result, a set of training samples is generally needed to obtain required information. An ML classifier is called supervised if it requires a set of training samples to estimate and determine the designed parameters prior to classification. For example, if the conditional class probability distribution is assumed to be Gaussian, the designed parameters for class ω_i will be the class mean μ_i and variance σ_i^2.

5. Experimental Results and Discussions

All ultrasonic images used in experiments were captured by a Toshiba Sonolayer SSA250A with PVE375 3.75 MHz (dynamic focusing) transducer at National Cheng Kung University Hospital. The images were transferred via a VFG frame grabber to a PC-AT PC and digitized into 256x512 pixels with 256 gray levels. The resulting digital images were then transmitted through NFS network system to a Sun Sparc II workstation where the proposed TFCM-supervised ML classification system was implemented with C program language. Figures 7(a-c) are sample images of normal liver, hepatitis and cirrhosis taken from intercoastal view, respectively. For each image an area of interest with 41x91 pixels is selected under the probe from 4.5-6.5 scale depth and a specific time-gain control. Each area of interest is chosed, if possible, to include solely liver tissue without major blood vessel or hepatic duct. The experiments were conducted based on 90 test images which will be classified into three liver disease classes. These liver images have proven by liver biopsy and equally divided into 3 groups, each of which has 30 cases. Four methods will be evaluated based on these 90 test images and compared in terms of classification rate and computing time.

We first analyze the classification rates of the four methods. Table 1 lists all the features selected by the forward sequential search algorithm for all the four methods and used in the classification procedures and their computing times. In Table 1 given below, the rows of tables represent the correct results proven by

biopsy and the columns of tables are classification resulting from classified techniques. From this Table 1, TFCM is the best among the four methods. It is found that the TFCM completely extracts the gray level gradient variation in the ultrasonic liver images for classification. The second best is Method 2 using the co-occurrence matrix. The result reveals that the disease changes of ultrasonic liver images are related to the gray level changes in liver images. The TS and SFM mainly measure some image properties such as coarseness or some specific arrangement of image pattern in a small area. Form the Table 1, The SFM and TS are the worst and their performances are nearly the same. We are not surprised with the results since these features generated by TS and SFM are not e nough to overcome the poor image quality of a small area in the ultrasonic liver images.

As far as computing time is concerned, the Table 1 reveal that TS requires the least time 2.98 seconds and CM is the slowest method requiring 51.56 seconds. Contrary to CM, the TFCM is better to generating texture features and has the best performance among other methods. It is our opinion that based on the classification rate and computing time, we can conclude that the TFCM may be the best candidate system for liver texture classification among all the methods examined in our experiments. Unlike the texture spectrum, we consider the connectivity of each texture unit to generate the feature number. In this feature number coding method, the permutation of the first-order and second-order connectivity of a texture unit do not change the feature number, since the feature number of a small area will persist when the estimated image has few rotation. Futhermore, In the past studies, conventional methods suffered the poor quality of ultrasonic liver images. In TFCM method, we use the maximum TFN entropy criterion to find the optimal the tolerance of gray level variation. Thus, the influence of the noises can be suppressed effectively. In spite of the fact that the performance of CM method is less than the TFCM method, it is found that the gray level changes of the ultrasonic liver image is valuable for classification. Thus, It is very interesting work in the future to combine the TFCM method with CM method.

6.Conclusion

In this paper, a TFCM classification system was designed to classify three classes of liver diseases. A new texture feature coding method (TFCM) was introduced into the system which transforms a liver image into a feature image where each pixel in the feature image is represented by a texture feature number (*TFN*) coded by TFCM. Based on the texture feature numbers in the feature image, a texture feature number histogram and co-occurrence matrix can be generated from which a set of texture feature descriptors is derived for texture classification. As for classification, a supervised maximum likelihood classifier is implemented. The performance of the proposed TFCM-supervised ML classification system was compared to the gray-level co-occurrence matrix method, statistical feature method and texture spectrum method. The experimental results conducted based on 90 test liver images showed that the TFCM-supervised ML classification system outperformed all other methods and correct classification rate could achieve as high as 83.3%.

Table 1. Features selected by the forward sequential search algorithm [7], computing time and correct classification rate.

Method	Feature Selectesd	Correct classificatio n rate	Comput- ing Time
CM	SE($\theta = 90^0$),DE($\theta = 0^0$), COR($\theta = 90^0$) ASM($\theta = 90^0$)	75.7%	51.56
TS	GS, MDS2,BWS and MHS	57.78%	3.489
SFM	Contrast, Coarseness and Periodicity Measure	55.67%	2.986
TFCM	Var, GLRS, Entropy and Similarity	83.3%	5.899

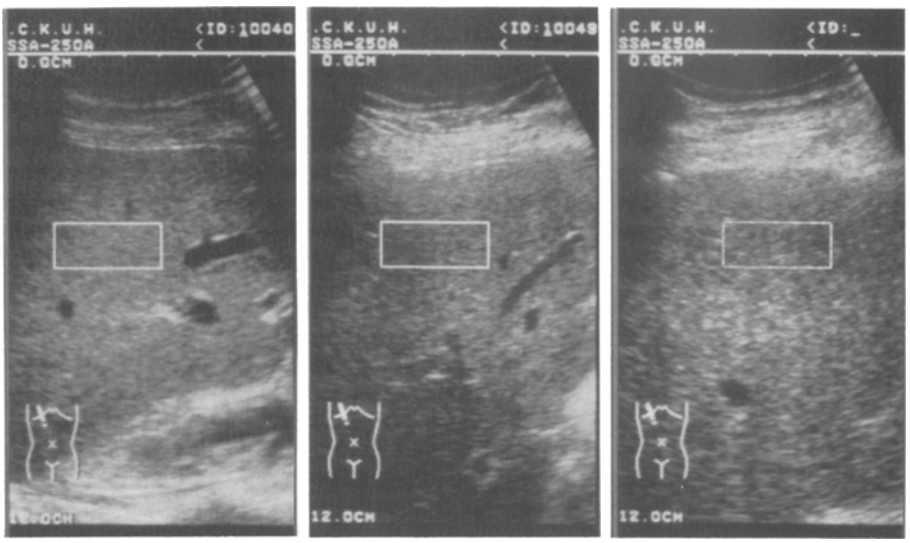

Figure 7(a). A case of normal liver (b). A case of liver hepatitis (c). A case of liver cirrhosis

7. Acknowledgment

The author would like to thank the National Science Council, R.O.C. under Grant No. NSC 84-2213-E-006-086 and the Department of Public Health under Grant No. DOH84-HR-416 for support of this work.

8. References

1. R.M. Haralick, K. Shanugan and I. Dinstein, "Texture features for image classification," *IEEE Trains. Syst. Man. Cybernet.* Vol 3, pp. 610-621, 1973.
2. A. Duerinckx, K. Rosenberg, D. Aufrichting, A Beuget, G. Kanel and S. Lottenberg."I"In vivio acoustic attention in liver correlation with blood tests and histology," Ultrasound in Med. and Biol., vol. 14, pp 405-413, 1988.
3. Y.N. Sun, H.T. Chiu and X.Z. Lin, "A computer system for the analysis of liver cirrhosis from ultrasonic images," *Chinese Journal of Medical and Biological Engineering,* Vol. 11, No. 2, pp. 119-135, 1991.
4. C.M. Wu, Y.C. Chen, and K.S. Hsieh, "Texture feature for classification of ultrasonic liver images," *IEEE Trans. Med. Imaging*, Vol. 11, No. 2, pp. 141-152, 1992.
5. C.M. Wu, and Y.C. Chen, "Statistical feature matrix for texture analysis," *Comput. Vision Graphic, Image Processing* , Vol. 54, No. 5, pp 407-419, 1992.
6. D.C. He and L. Wang. "T"Texture features based on texture spectrum," *Pattern Recognition*, Vol. 24, No. 5, pp.391-399, 1991.
7. D.C. He, L. Wang and J. Guibert, "Texture discrimination based on an optimal utilization of texture features," *Pattern Recognition*, Vol. 21, No. 2, pp141-146, 1988.